

Original article:

**PROTEOMIC ANALYSIS OF HEPATIC EFFECTS OF OKADAIC ACID
IN HEPARG HUMAN LIVER CELLS**

Leonie T.D. Wuerger^{ID}, Greta Birkholz^{ID}, Axel Oberemm^{ID}, Holger Sieg*^{ID},
Albert Braeuning^a^{ID}

German Federal Institute for Risk Assessment, Department of Food Safety,
Max-Dohrn-Str. 8-10, 10589 Berlin, Germany

* **Corresponding author:** Holger Sieg, German Federal Institute for Risk Assessment,
Department of Food Safety, Max-Dohrn-Str. 8-10, 10589 Berlin, Germany;
E-mail: holger.sieg@bfr.bund.de

<https://dx.doi.org/10.17179/excli2023-6458>

This is an Open Access article distributed under the terms of the Creative Commons Attribution License
(<http://creativecommons.org/licenses/by/4.0/>).

ABSTRACT

The marine biotoxin okadaic acid (OA) is produced by dinoflagellates and enters the human food chain by accumulating in the fatty tissue of filter-feeding shellfish. Consumption of highly contaminated shellfish can lead to diarrhetic shellfish poisoning. However, apart from the acute effects in the intestine, OA can also provoke toxic effects in the liver, as it is able to pass the intestinal barrier into the blood stream. However, molecular details of OA-induced hepatotoxicity are still insufficiently characterized, and especially at the proteomic level data are scarce. In this study, we used human HepaRG liver cells and exposed them to non-cytotoxic OA concentrations for 24 hours. Global changes in protein expression were analyzed using 2-dimensional gel electrophoresis in combination with mass-spectrometric protein identification. The results constitute the first proteomic analysis of OA effects in human liver cells and indicate, amongst others, that OA affects the energy homeostasis, induces oxidative stress, and induces cytoskeletal changes.

Keywords: Okadaic acid, HepaRG cells, liver proteome

INTRODUCTION

Okadaic acid (OA) is one of the main toxins to cause diarrhetic shellfish poisoning (DSP). It is produced by dinoflagellates of the genus *dinophysis* and *prorocentrum* (EFSA, 2008). These dinoflagellates probably produce the toxin to gain an advantage against other microalgae (Gong et al., 2021). Under optimal conditions, OA-expressing dinoflagellates can explosively grow, leading to so-called harmful algae blooms. Due to climate change and the industrial waste of humans, the occurrence of harmful algae blooms has

significantly increased in the last years, leading to an increase in OA occurrence (Van Dolah, 2000). OA is very lipophilic, thereby accumulating in the fatty tissue of filter-feeding shellfish, through which they can also enter the human food chain. In humans, OA can cause DSP, which leads to severe gastrointestinal symptoms, like vomiting, diarrhea and stomach pain. Based on that, the European Union has implemented a limit of 160 OA equivalents/kg shellfish meat, based on the acute reference dose of 0.3 µg OA equivalents/kg body weight (FAO, 2004).

While the most extensively researched acute effects of OA intoxication are observed in the intestine, effects on other organs have been investigated and understood much less. However, it was shown that OA is distributed throughout the whole body *in vivo* and that it has a particularly long retention time in the liver (Matias et al., 1999; Ito et al., 2002). Furthermore, OA is able to inhibit several protein phosphatases, mainly protein phosphatase 1 and 2A (Bialojan and Takai, 1988). Therefore, it has the potential to severely influence kinase- and phosphorylation-dependent signaling pathways in the liver. There is also evidence that OA acts as a potent tumor promoter in animals (Jiménez-Cárcamo et al., 2020; Messner et al., 2006) and it might be the cause of cancer cases reported in epidemiological studies (Cordier et al., 2000; Lopez-Rodas et al., 2006; Manerio et al., 2008). OA was also found to be cytotoxic in several different cell lines, including liver cells (Ferron et al., 2014; Fessard et al., 1996; Le Hégarat et al., 2006; Rubiolo et al., 2011). The toxin is furthermore able to interfere with xenobiotic metabolism in the liver by inhibiting several enzymes of hepatic biotransformation (Vieira et al., 2013; Wuerger et al., 2022). Apart from that, the information on the effects of OA on the liver is very limited.

In a comparative proteomics 2D-PAGE analysis of mouse liver, Wang et al. found 46 deregulated proteins involved in macromolecular metabolism, molecular chaperone/stress response, apoptosis, and cytoskeleton formation after chronic exposure to OA (Wang et al., 2021). This study in mice is, to the best of our knowledge, the only available study describing changes to the liver proteome after OA exposure. The only other proteomic study with OA is reported in a publication from the same research group and describes proteomic alterations in mouse small intestine after a single oral dose of OA (Wang et al., 2012). Technically, both studies were performed using gel-based 2-dimensional separation of proteins, followed by mass-spectrometric identification of deregulated proteins.

In order to close the existing knowledge gap regarding the effects of OA on human liver cells, we conducted a proteomic study of human HepaRG liver cells exposed to different concentrations of OA. HepaRG cells are able to differentiate into hepatocyte-like cells, which express a variety of liver-specific markers and xenobiotic-metabolizing enzymes at a level similar to primary human hepatocytes (Kanebratt and Andersson, 2008; Tascher et al., 2019). 2-dimensional gel electrophoresis and subsequent mass-spectrometric protein identification was chosen in order to generate data suitable for a direct comparison to the results from the two studies by Wang and co-workers (Wang et al., 2012, 2021).

MATERIALS AND METHODS

Chemicals

OA was purchased from Enzo Life Sciences GmbH (Loerrach, Germany). All other standard chemicals and materials were purchased either from Sigma-Aldrich (Taufkirchen, Germany) or Roth (Karlsruhe, Germany) in the highest available purity.

Cell cultivation

HepaRG cells (Biopredic International, Saint-Grégoire, France) were cultivated at 37 °C for 14 days in William's E medium supplemented with 10 % fetal bovine serum (FBS), 5 µg/mL insulin (medium and both supplements from PAN-Biotech GmbH, Aidenbach, Germany), 50 µM hydrocortisone hemisuccinate (Sigma Aldrich, Taufkirchen, Germany), and with 100 U/mL penicillin and 100 µg/mL streptomycin (Capricorn Scientific, Ebsdorfergrund, Germany). After 14 days, the medium was supplemented with 1 % dimethyl sulfoxide (DMSO) for 2 days to start differentiation of the cells. After that, the DMSO content was increased to 1.7 % for another 12 days. The medium was then changed to serum-free assay medium (SFM), which was adapted from Klein et al. (2014). SFM consisted of William's E medium without phenol red (PAN-Biotech GmbH, Aidenbach,

Germany), supplemented with 100 U/mL penicillin and 100 µg/mL streptomycin, 2.5 µM hydrocortisone hemisuccinate, 10 ng/mL human hepatocyte growth factor (Biomol GmbH, Hamburg, Germany), 2 ng/mL mouse epidermal growth factor (Sigma Aldrich, Taufkirchen, Germany), and 0.5 % DMSO. Cells were incubated with 33 nM OA, 100 nM OA or the respective solvent control for 24 hours.

Cell viability testing

Cell viability testing was conducted as previously reported (Wuerger et al., 2022). In short, 9×10^3 cells/well were seeded in 96-well plates and cells were cultivated as described above. Cells were then incubated with different OA concentrations for 24 h. Cell viability was subsequently determined using the tetrazolium dye 3-(4,5-dimethylthiazol-2-yl)-2,5-diphenyltetrazolium bromide (MTT; Biomol GmbH, Hamburg, Germany).

Protein extraction

The HepaRG cells were washed in ice-cold PBS and then scraped in PBS. The cells were then centrifuged (5 min, 2000 x g, 4 °C). For protein extraction from HepaRG cell pellets, RIPA lysis buffer (pH 7.5; 50 mM Tris-HCl, 150 mM NaCl, 2 µM EGTA, 0.1 % sodium dodecyl sulfate (SDS), and 0.5 % desoxycholic acid) containing 1:50 protease inhibitor (Complete Protease Inhibitor Cocktail Tablets, Roche, Mannheim, Germany) and 1 % Triton X-100 was used. The cells were lysed by rotating at 4 °C for 15 min, and homogenization was carried out using an ultrasonic homogenizer (Sonopuls HD 2070, BANDELIN electronic GmbH & Co. KG, Berlin, Germany, 25 % power, pulse 2). The homogenized lysates were then centrifuged at 4 °C and 13,200 x g for 30 min. The supernatant was collected and stored at -80 °C. The protein content in the resulting supernatants was determined using the Bradford assay according to the manual of the Bio-Rad protein assay (Bio-Rad Laboratories GmbH, Feldkirchen, Germany) against a bovine serum albumin standard curve.

2-dimensional gel electrophoresis

2-dimensional gel electrophoresis was carried out according to the protocol by Görg et al. (2000). In brief, isoelectric focusing (IEF) was done using 24-cm IPG gel strips, which were loaded with 150 µg protein; gel running conditions are detailed in Görg et al. (2000). After equilibration, SDS-polyacrylamide gel electrophoresis was performed with laboratory-made 12.5 % acrylamide gels. Subsequent to fixation in aqueous acetic acid/ethanol, gel staining was performed using Ruthenium II Tris solution (pH 7; 20 mM potassium tetrachloroaurate (III), 0.16 mM bathophenanthrolinedisulfonic acid disodium salt hydrate, 96 mM sodium ascorbate). The stained gels were scanned in a Molecular Imager Versadoc MP 4000 (Bio-Rad Laboratories GmbH, Feldkirchen, Germany), with an excitation wavelength at 450 nm and emission wavelength at 605 nm. Analysis of the images was carried out using ProteinMine software (Scimagix, San Mateo, CA, USA) with a minimal spot size of 8 and a sensitivity of 35. The generated data was then analyzed in R (R Core Team) using an internal script that uses the Wilcoxon Rank sum test to determine the differentially expressed protein spots (cutoffs: $p \leq 0.01$ and $|\log_2 \text{ratio}| \geq 0.5$). Spots were included if detected in 2 out of 3 biological and in 2 out of 4 technical replicates.

Mass-spectrometric protein identification

The annotated protein spots were identified using MALDI mass spectrometry. The spots were cut from the gels and dehydrated using acetonitrile (Merck KGaA, Darmstadt, Germany). The dehydrated gel spots were then rehydrated for 30 minutes at 4 °C using a trypsin solution (0.425 µM trypsin (Roche, Mannheim, Germany) in 50 mM ammonium bicarbonate (pH 8, Sigma Aldrich, Taufkirchen, Germany)). After 30 minutes, the retaining solution was discarded and the gel pieces were put into a 50 mM ammonium bicarbonate solution (pH 8; Sigma Aldrich, Taufkirchen, Germany). The spots were di-

gested over night at 37 °C. Then, trifluoroacetic acid (Merck KGaA, Darmstadt, Germany) was added to the spots to extract the peptides. Each spot was analyzed using an Ultraflex II MALDI-TOF/TOF mass spectrometer (Bruker Daltonics, Billerica, Massachusetts, USA). The corresponding proteins for each spot were then identified using MASCOT (Matrix Science, London, UK). Proteins were sorted into categories related to different cellular processes using the UniProt database (<https://www.uniprot.org/2023>).

RESULTS

To assess changes in the liver proteome after exposure to OA, we analyzed the proteome from differentiated HepaRG cells after exposure to non-toxic concentrations of OA using 2-dimensional gel electrophoresis. Non-toxic concentrations of OA were determined using the MTT assay. From the data shown in Supplementary Figure 1, 33 nM and 100 nM were selected as moderate and high non-toxic OA concentrations, respectively. After incubation with OA, 2D gels were run as described in the “Methods” section. Figure 1 depicts representative gels of each treatment group. Gels were stained using Ruthenium II Tris solution. The spot patterns on the gels were then detected using the software ProteinMine and analyzed using the Wilcoxon

rank sum test. Only spots that were detected in at least two of the three biological and in two of the four technical replicates were considered for the analysis. We were able to find 68 significantly deregulated protein spots in the 33 nM OA group ($p \leq 0.01$ and $|\log_2 \text{ratio}| \geq 0.5$), 34 of which were upregulated and 34 downregulated. In the 100 nM OA group we detected 65 downregulated protein spots and 55 upregulated spots, which adds up to a total of 120 deregulated spots (Figure 2A). 34 protein spots were overlapping between both groups (Figure 2B). The combination of a comparably strict p value and a moderate fold change cutoff was chosen to allow for the identification of only slightly deregulated proteins, while at the same time avoiding false-positive results. The individual proteins present in the deregulated protein spots were then identified using MALDI-MS. 41 proteins were identified for the 33 nM group (identification rate 60 %) and 84 proteins for the 100 nM group (identification rate 70 %), with 21 proteins that were found in both groups (Figure 2C). The most upregulated protein was peroxiredoxin 6, which was found in the 100 nM treatment group (Table 1). The 15 most upregulated proteins are listed in Table 1. The most downregulated protein was isocitrate dehydrogenase (NADP) 1, which was found in the 33 nM treatment group (Table 2). The 15 most down-

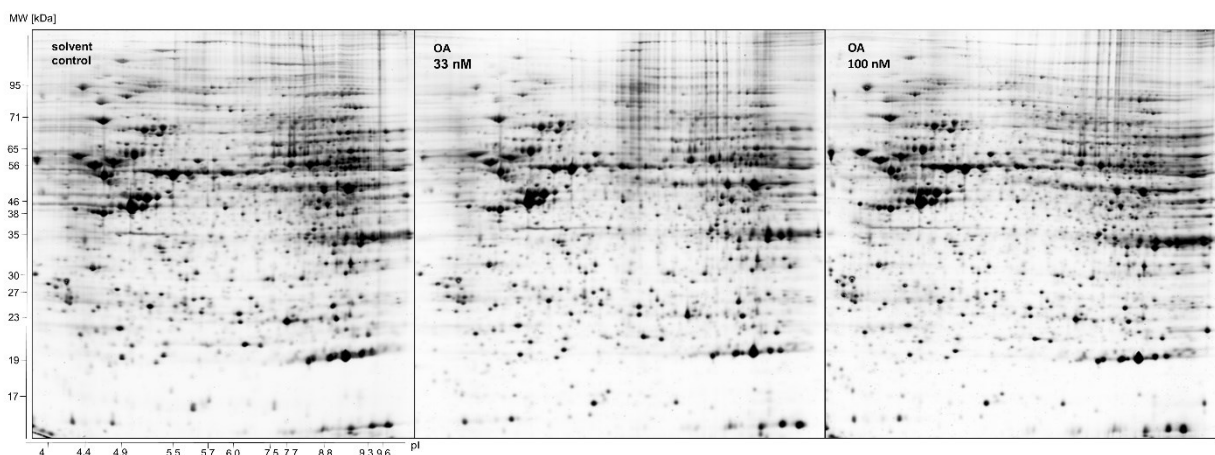


Figure 1: Representative gels of separated proteins from HepaRG cells incubated with 33 or 100 nM OA for 24 h. HepaRG cells were lysed, and proteins were extracted. Proteins were first separated using isoelectric focusing and then further using SDS-PAGE. Gels were stained using Ruthenium II Tris solution, n=3.

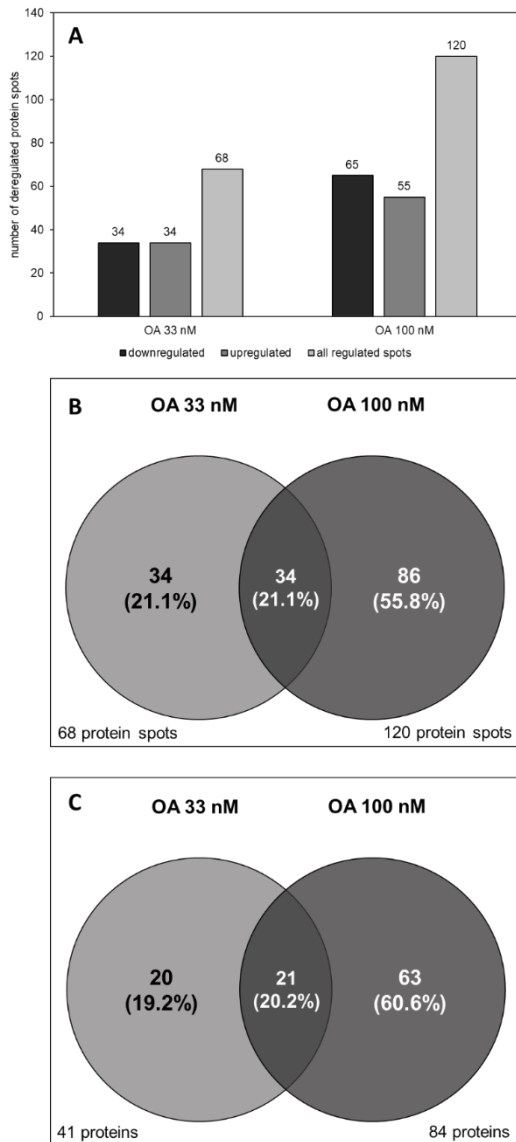


Figure 2: Deregulated protein spots and identified deregulated proteins in OA-treated HepaRG cells. Proteins were isolated from HepaRG cells incubated with 33 or 100 nM OA for 24 h. Proteins were then separated using 2D gel electrophoresis and deregulated protein spots were identified using the Wilcoxon Rank sum test ($p \leq 0.01$ and $|\log_2 \text{ratio}| \geq 0.5$). **(A)** Total numbers of up- and downregulated protein spots. **(B)** Venn diagram visualization of the overlap of deregulated protein spots between the treatment groups, presented in absolute numbers and percentages. **(C)** The proteins corresponding to each spot were identified using MALDI-MS; the diagram shows the numbers and percentages of identified proteins in the treatment groups and their overlap.

regulated proteins are listed in Table 2. The full list of deregulated proteins is contained in Supplementary Table 1. Please note that individual proteins might be present and detected as different spots on the gels, for example when a protein occurs in different post-translational modifications. Therefore, appearance of a certain protein in the lists for up- and downregulated proteins does not invalidate the data, but points towards a shift between protein isoforms. Moreover, changes detected by 2-DIGE/MALDI-MS might not be reflected by changes in the overall amount of a protein (i.e., the sum of all differently modified forms of it).

The identified proteins were assigned to different cellular functions and processes using the UniProt database (Figure 3). It was observed that 25 % of all identified proteins were associated with energy homeostasis (for example, PDHB, GLUL and ETFA), 15 % were related to protein metabolism (for example, EEF2, EIF4H or UBQLN1), and 13 % were chaperones or proteins involved in oxidative stress-related processes (for example, HSP90B1, HSPA4 or PRDX6; Figure 3A). As one quarter of all deregulated proteins were connected with energy homeostasis, we further assigned them to the different pathways of the energy metabolism (Figure 3B). The largest group of the aforementioned proteins (41 %) take part in the metabolisms of lipids and/or fatty acids (for example ACAT1, APOE or HEXA), while another 19 % were also associated to carbohydrate metabolism (for example, PGM1, TALDO1, ALDOC) and another 18 % were proteins of the amino acid metabolism (for example, ACY1, GLUL or HIBCH). This indicates that both, lipid and carbohydrate metabolism, are substantially affected by OA in HepaRG cells.

Table 1: The 15 most prominently upregulated proteins in all samples. Proteins were isolated from HepaRG cells incubated with 33 or 100 nM OA for 24 h. Proteins were then separated using 2D gel electrophoresis and deregulated proteins were identified using MALDI-MS.

Protein symbol	UniProt accession	Protein name	Fold change (log ₂)	p-value	Treatment group
PRDX6	Q13162	Peroxiredoxin 6	1.872	2.84E-06	OA 100 nM
ZYX	Q15942	Zyxin	1.752	5.67E-05	OA 100 nM
EIF4H	Q15056	Eukaryotic translation initiation factor 4H	1.727	6.18E-03	OA 100 nM
PCNA	P12004	Proliferating cell nuclear antigen	1.530	7.66E-03	OA 100 nM
ZYX	Q15942	Zyxin	1.335	2.72E-04	OA 100 nM
PCNA	P12004	Proliferating cell nuclear antigen	1.354	9.99E-04	OA 33 nM
SLC9A3R1	O14745	SLC9A3 Regulator 1	1.284	1.23E-03	OA 100 nM
PDIA6	Q15084	Protein disulfide-isomerase A6	1.280	7.97E-03	OA 100 nM
FGB	P02675	Fibrinogen beta chain	1.277	2.97E-03	OA 100 nM
EEF2	P13639	Elongation factor 2	1.266	3.71E-04	OA 100 nM
PCNA	P12004	Proliferating cell nuclear antigen	1.258	6.80E-06	OA 33 nM
ANXA1	P04083	Annexin A1	1.190	8.23E-05	OA 100 nM
PCNA	P12004	Proliferating cell nuclear antigen	1.174	3.09E-06	OA 100 nM
ALDOC	P09972	Fructose-bisphosphate aldolase C	1.146	2.29E-03	OA 100 nM
ALDH1L1	O75891	Aldehyde dehydrogenase 1 family member L1	1.145	7.66E-03	OA 100 nM

Table 2: The 15 most prominently downregulated proteins in all samples. Proteins were isolated from HepaRG cells incubated with 33 or 100 nM OA for 24 h. Proteins were then separated using 2D gel electrophoresis and deregulated proteins were identified using MALDI-MS.

Protein symbol	UniProt accession	Protein name	Fold change (log ₂)	p-value	Treatment group
IDH1	O75874	Isocitrate dehydrogenase (NADP) 1	-1.971	6.50E-04	OA 33 nM
HP	P00738	Haptoglobin	-1.544	2.96E-06	OA 33 nM
HSP90B1	P14625	Heat shock protein 90 beta family member 1	-1.539	1.98E-05	OA 100 nM
HP	P00738	Haptoglobin	-1.538	1.98E-05	OA 100 nM
HNRNPK	P61978	Heterogeneous nuclear ribonucleoprotein K	-1.522	7.40E-07	OA 100 nM
GLUL	P61978	Glutamine synthetase	-1.462	2.65E-05	OA 100 nM
TUFM	P49411	Tu translation elongation factor, mitochondrial	-1.380	1.41E-04	OA 100 nM
ACO2	Q99798	Aconitase 2	-1.371	5.35E-03	OA 100 nM
SEPTIN2	Q15019	Septin 2	-1.145	1.49E-03	OA 33 nM
GSTA1	P08263	Glutathione S-transferase A1	-1.109	2.83E-03	OA 33 nM
TKFC	Q3LXA3	Triokinase/FMN cyclase	-1.102	9.99E-04	OA 33 nM
MAT1A	Q00266	Methionine adenosyltransferase 1A	-1.099	5.48E-03	OA 100 nM
IMMT	Q16891	MICOS complex subunit MIC60	-1.079	6.43E-03	OA 100 nM
PGM1	P36871	Phosphoglucomutase 1	-1.054	9.69E-03	OA 100 nM
GLUL	P15104	Glutamine synthetase	-1.053	1.48E-06	OA 33 nM

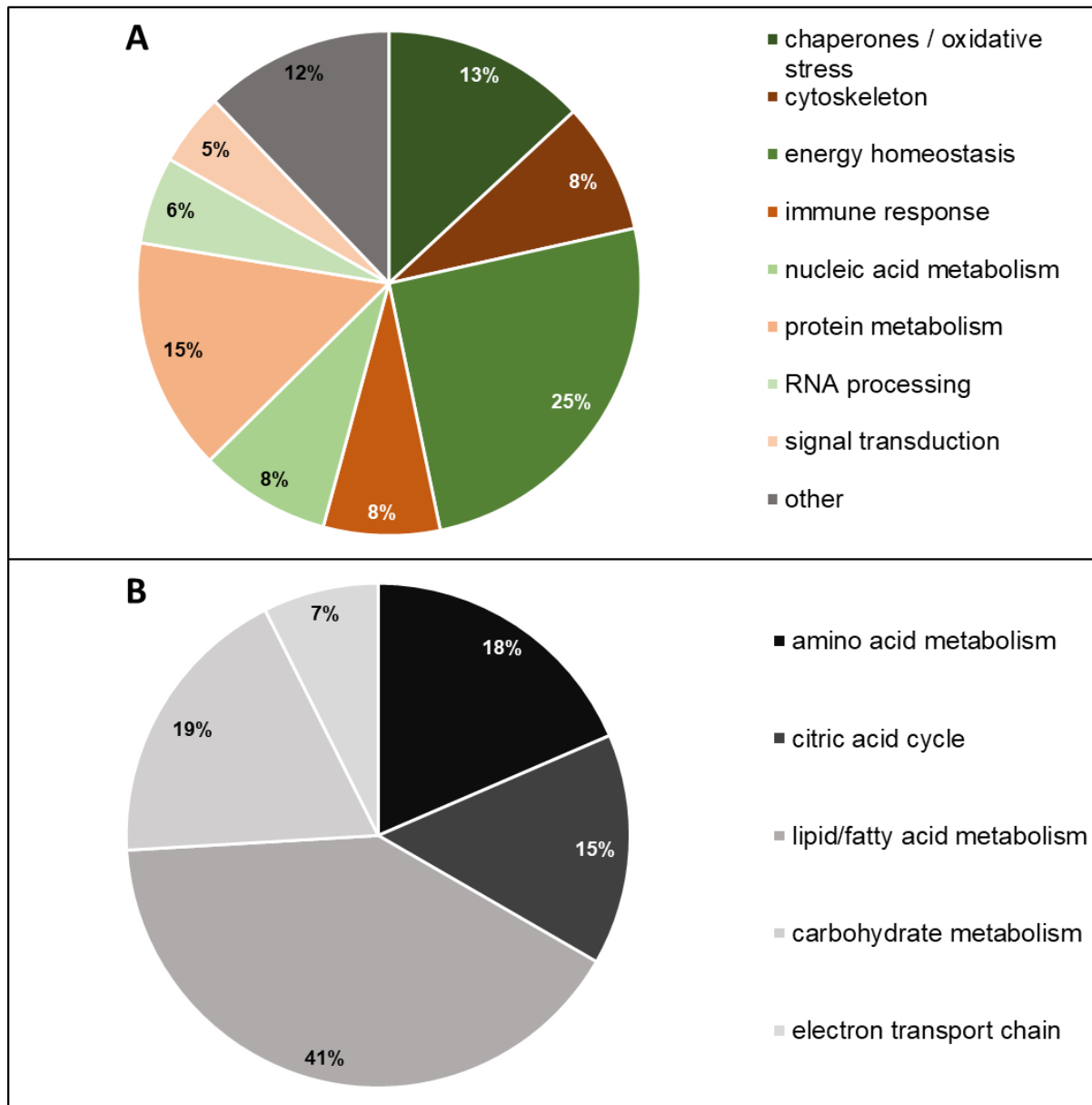


Figure 3: Grouping of identified OA-regulated proteins according to their cellular functions. **(A)** Distribution of the proteins between different cellular functions and processes according to the UniProt database. **(B)** Detailed functional grouping of the proteins related to energy homeostasis

DISCUSSION

Even though OA has mostly been recognized for its acute effects in the gut, but is able to pass the intestinal barrier and reach the liver, where it has a long retention time (Ito et al., 2002, Matias et al., 1999, Dietrich et al., 2019). Nonetheless, only few hepatic effects of OA have been characterized so far. For example, a mechanism for the OA-dependent downregulation of drug metabolism-related

enzymes in human liver cells has been recently deciphered (Wuerger et al., 2022, 2023). Not much, however, is known about the overall proteomic response of liver cells to OA, and only a single proteomic study with mouse liver after chronic exposure to OA has been published in the past (Wang et al., 2021). Additional proteomic information comes from a study with mouse intestine (Wang et al., 2012), and a limited proteomic data set has also been generated from isolated lipid

rafts of a human neuroblastoma cell line (Opsahl et al., 2013). We aimed at closing the knowledge gap regarding hepatic proteomic effects of OA by using a well-established *in vitro* model of human liver, HepaRG cells, in combination with gel-based protein separation and mass-spectrometric protein identification. This was done in order to generate a proteomic data set allowing the comparison with the aforementioned published data based on a technically comparable approach. HepaRG cells were incubated with non-toxic doses of OA, to detect OA-specific alterations and to avoid the occurrence of unspecific cytotoxic responses of the cells. Therefore, the present study is the first to provide an unbiased proteomic analysis of OA-induced alterations in human cells, and the first proteomic study of hepatic OA effects conducted with human cells. In our study, a total number of 104 proteins were identified, as compared to 46 proteins in mouse liver and 58 proteins in mouse intestine, respectively, in previous studies (Wang et al., 2012, 2021). Thus, our results constitute a substantial improvement of knowledge regarding the cellular effects of OA at the protein level.

Supplementary Table 1 lists the deregulated proteins identified in our analysis, along with information whether the respective proteins (i.e., their direct murine orthologs, or similar isoforms) have been identified as OA-regulated in the two aforementioned publications by Wang and co-workers. In fact, congruence of 34 entries (28 %) from our HepaRG-derived protein list with proteins previously identified as being affected by OA in mouse liver or intestine was noted (Supplementary Table 1). This high level of congruence, despite the species difference and the differences in study design and analytical workflow, substantiates the validity of the results obtained in our study.

One quarter of the OA-regulated proteins identified in this study were functionally associated with energy homeostasis, and most of them are part of pathways related to lipid or fatty acid metabolism. The liver is one of

the most important organs for energy homeostasis in the human body (Rui, 2014). It is the central organ for fatty acid metabolism. This includes, among other processes, the *de novo* synthesis and also the elimination of fatty acids (Alves-Bezerra and Cohen, 2017). It has been shown that OA is able to promote lipolysis, thereby interfering with fatty acid metabolism (He et al., 2006). The liver furthermore plays a central role in glucose metabolism, including glycogenesis, glycogenolysis, glycolysis and gluconeogenesis (Han et al., 2016). Previous data indicate that OA is able to interfere with glucose metabolism in hepatocytes by increasing gluconeogenesis and glucose output (Louzao et al., 2005). Thus, the identification of a high percentage of OA-deregulated proteins as associated with fat and energy metabolism is in line with previous data. Only one core component of glycolysis (ALDOC) was found affected by OA in our analysis, while a number of proteins related to the tricarboxylic acid cycle (ACO2, IDH1, PDHA1, PDHB) were also identified as altered in OA-treated HepaRG cells.

Exposure to OA is able to induce inflammatory responses. For example, OA is able to activate the expression and release of different proinflammatory cytokines *in vitro* (Del Campo et al., 2017; Suuronen et al., 2006; Tchiveleketete et al., 2022; Wuerger et al., 2023). An increase of IL-1 β caused by OA was furthermore detected in rat brains *in vivo* (Kamat et al., 2012). OA is furthermore a known inducer of reactive oxygen species (ROS) (Schmidt et al., 1995; Túnez et al., 2003), and therefore a cellular ROS-related response following OA exposure is to be expected. 13 % of the identified proteins in our analysis were chaperones or part of the cellular response to oxidative stress. Similar results were also obtained by Wang et al., where a comparable percentage of the identified proteins in mouse liver was related to oxidative stress and/or chaperone function (Wang et al., 2021).

Another noteworthy aspect of our results is that 8 % of the identified proteins were part of the cytoskeleton. Wang et al. also found an

effect of OA on the cytoskeleton in mouse liver, with 13 % of their identified proteins being part of it (Wang et al., 2021). In the second study by Wang et al., the authors also found a large number of the regulated proteins in mouse intestine to be part of the cytoskeleton (Wang et al., 2012). The cytoskeleton is, among others, responsible for the overall integrity of the cell, cell adhesion, and cell-cell contacts (Huber et al., 2013). One of the known main targets of OA is the cytoskeleton. This leads, for example, to a disruption of tight junctions or actin filaments (Dietrich et al., 2019; Opsahl et al., 2013; Huang et al., 2023). Our data provide additional evidence for effects of OA on the cytoskeleton and thus broaden our knowledge on this aspect of the molecular toxicity of OA.

In conclusion, our data confirm and substantially extend our knowledge regarding proteomic effects of okadaic acid in mammalian cells and, for the first time, provide insight into hepatocellular proteomic effects of OA in human cells.

Author contributions

LW 1,2,3,4
GB 1,2
AO 1,2
HS 3,4
AB 3,4,5

- 1: Performed experiments
- 2: Data evaluation
- 3: Writing the manuscript
- 4: Project planning
- 5: Supervision and funding

Declaration of competing interest

We declare that there is no competing interest.

Acknowledgment

We would like to thank Christine Meckert for technical assistance. This project was supported by the German Federal Institute for Risk Assessment, Germany (project 1322-824).

REFERENCES

- Alves-Bezerra M, Cohen DE. Triglyceride metabolism in the liver. *Compr Physiol.* 2017;8(1):1-8. doi: 10.1002/cphy.c170012.
- Bialojan C, Takai A. Inhibitory effect of a marine-sponge toxin, okadaic acid, on protein phosphatases. Specificity and kinetics. *Biochem J.* 1988;256:283-90. doi: 10.1042/bj2560283.
- Cordier S, Monfort C, Miossec L, Richardson S, Belin C. Ecological analysis of digestive cancer mortality related to contamination by diarrhetic shellfish poisoning toxins along the coasts of France. *Environ Res.* 2000;84:145-50. doi: 10.1006/enrs.2000.4103.
- Del Campo M, Zhong TY, Tampe R, García L, Lagos N. Sublethal doses of dinophysistoxin-1 and okadaic acid stimulate secretion of inflammatory factors on innate immune cells: Negative health consequences. *Toxicol.* 2017;126:23-31. doi: 10.1016/j.toxicol.2016.12.005.
- Dietrich J, Grass I, Günzel D, Herek S, Braeuning A, Lampen A, et al. The marine biotoxin okadaic acid affects intestinal tight junction proteins in human intestinal cells. *Toxicol Vitro.* 2019;58:150-60. doi: 10.1016/j.tiv.2019.03.033.
- EFSA. Scientific Opinion of the Panel on Contaminants in the Food chain on a request from the European Commission on marine biotoxins in shellfish—okadaic acid and analogue. *EFSA J.* 2008;589:1-62. doi: 10.2903/j.efsa.2008.589.
- FAO. Marine biotoxins. *FAO Food Nutr Pap.* 2004;80:53-92.
- Ferron PJ, Hogeveen K, Fessard V, Le Hégarat L. Comparative analysis of the cytotoxic effects of okadaic acid-group toxins on human intestinal cell lines. *Mar Drugs.* 2014;12:4616-34. doi: 10.3390/md12084616.
- Fessard V, Grosse Y, Pfohl-Leszkowicz A, Puiseux-Dao S. Okadaic acid treatment induces DNA adduct formation in BHK21 C13 fibroblasts and HESV keratinocytes. *Mutat Res.* 1996;361:133-41. doi: 10.1016/s0165-1161(96)90248-4.
- Görg A, Obermaier C, Boguth G, Harder A, Scheibe B, Wildgruber R, et al. The current state of two-dimensional electrophoresis with immobilized pH gradients. *Electrophoresis.* 2000;21:1037-53. doi: 10.1002/(sici)1522-2683(20000401)21:6<1037::Aid-elps1037>3.0.Co;2-v.

- Gong Y, Zhang K, Geng N, Wu M, Yi X, Liu R, et al. Molecular mechanisms of zooplanktonic toxicity in the okadaic acid-producing dinoflagellate *Prorocentrum lima*. *Environ Pollut*. 2021;279:116942. doi: 10.1016/j.envpol.2021.116942.
- Han HS, Kang G, Kim JS, Choi BH, Koo SH. Regulation of glucose metabolism from a liver-centric perspective. *Exp Mol Med*. 2016;48(3):e218. doi: 10.1038/emm.2015.122.
- He J, Jiang H, Tansey JT, Tang C, Pu S, Xu G. Calyculin and okadaic acid promote perilipin phosphorylation and increase lipolysis in primary rat adipocytes. *Biochim Biophys Acta*. 2006;1761:247-55. doi: 10.1016/j.bbali.2006.02.001.
- Huang L, Liu B, Yu XW, Pan GQ, Xu JY, Yan D, et al. Rat tight junction proteins are disrupted after sub-chronic exposure to okadaic acid. *Environ Sci Pollut Res Int*. 2023;30:62201-12. doi: 10.1007/s11356-023-26471-x.
- Huber F, Schnauß J, Rönicke S, Rauch P, Müller K, Fütterer C, et al. Emergent complexity of the cytoskeleton: from single filaments to tissue. *Adv Phys*. 2013; 62:1-112. doi: 10.1080/00018732.2013.771509.
- Ito E, Yasumoto T, Takai A, Imanishi S, Harada K. Investigation of the distribution and excretion of okadaic acid in mice using immunostaining method. *Toxicol*. 2002;40:159-65. doi: 10.1016/s0041-0101(01)00207-0.
- Jiménez-Cárcamo D, García C, Contreras HR. Toxins of okadaic acid-group increase malignant properties in cells of colon cancer. *Toxins (Basel)*. 2020;12(3):179. doi: 10.3390/toxins12030179.
- Kamat PK, Tota S, Rai S, Swarnkar S, Shukla R, Nath C. A study on neuroinflammatory marker in brain areas of okadaic acid (ICV) induced memory impaired rats. *Life Sci*. 2012;90:713-20. doi: 10.1016/j.lfs.2012.03.012.
- Kanebratt KP, Andersson TB. Evaluation of HepaRG cells as an in vitro model for human drug metabolism studies. *Drug Metab Dispos*. 2008;36:1444-52. doi: 10.1124/dmd.107.020016.
- Klein S, Mueller D, Schevchenko V, Noor F. Long-term maintenance of HepaRG cells in serum-free conditions and application in a repeated dose study. *J Appl Toxicol*. 2014;34:1078-86. doi: 10.1002/jat.2929.
- Le Hégarat L, Jacquin AG, Bazin E, Fessard V. Genotoxicity of the marine toxin okadaic acid, in human Caco-2 cells and in mice gut cells. *Environ Toxicol*. 2006;21:55-64. doi: 10.1002/tox.20154.
- Lopez-Rodas V, Maneiro E, Martinez J, Navarro M, Costas E. Harmful algal blooms, red tides and human health: Diarrhetic shellfish poisoning and colorectal cancer. *An R Acad Farm*. 2006;72:391-408.
- Louzao MC, Vieytes MR, Botana LM. Effect of okadaic acid on glucose regulation. *Mini Rev Med Chem*. 2005;5:207-15. doi: 10.2174/1389557053402747.
- Manerio E, Rodas VL, Costas E, Hernandez JM. Shellfish consumption: A major risk factor for colorectal cancer. *Medical Hypotheses*. 2008;70:409-12. doi: 10.1016/j.mehy.2007.03.041.
- Matias WG, Traore A, Creppy EE. Variations in the distribution of okadaic acid in organs and biological fluids of mice related to diarrhoeic syndrome. *Hum Exp Toxicol*. 1999;18:345-50. doi: 10.1191/096032799678840156.
- Messner DJ, Romeo C, Boynton A, Rossie S. Inhibition of PP2A, but not PP5, mediates p53 activation by low levels of okadaic acid in rat liver epithelial cells. *J Cell Biochem*. 2006;99:241-55. doi: 10.1002/jcb.20919.
- Opsahl JA, Ljostveit S, Solstad T, Risa K, Roepstorff P, Fladmark KE. Identification of dynamic changes in proteins associated with the cellular cytoskeleton after exposure to okadaic acid. *Mar Drugs*. 2013;11:1763-82. doi: 10.3390/md11061763.
- Rubiolo JA, López-Alonso H, Vega FV, Vieytes MR, Botana LM. Okadaic acid and dinophysin toxin 2 have differential toxicological effects in hepatic cell lines inducing cell cycle arrest, at G0/G1 or G2/M with aberrant mitosis depending on the cell line. *Arch Toxicol*. 2011;85:1541-50. doi: 10.1007/s00204-011-0702-5.
- Rui L. Energy metabolism in the liver. *Compr Physiol*. 2014;4:177-97. doi: 10.1002/cphy.c130024.
- Schmidt KN, Traenckner EB, Meier B, Baeuerle PA. Induction of oxidative stress by okadaic acid is required for activation of transcription factor NF-kappa B. *J Biol Chem*. 1995;270:27136-42. doi: 10.1074/jbc.270.45.27136.
- Suuronen T, Huuskonen J, Nuutinen T, Salminen A. Characterization of the pro-inflammatory signaling induced by protein acetylation in microglia. *Neurochem Int*. 2006;49:610-8. doi: 10.1016/j.neuint.2006.05.001.
- Tascher G, Burban A, Camus S, Plumel M, Chanon S, Le Guevel R, et al. In-depth proteome analysis highlights HepaRG cells as a versatile cell system surrogate for primary human hepatocytes. *Cells*. 2019;8(2):192. doi: 10.3390/cells8020192.

- Tchivelekete GM, Almarhoun M, Cao Y, Zhou X, Martin PE, Shu X. Evaluation of okadaic acid toxicity in human retinal cells and zebrafish retinas. *Toxicology*. 2022;473:153209. doi: 10.1016/j.tox.2022.153209.
- Túnez I, Muñoz Mdel C, Feijóo M, Muñoz-Castañeda JR, Bujalance I, Valdelvira ME, et al. Protective melatonin effect on oxidative stress induced by okadaic acid into rat brain. *J Pineal Res*. 2003;34:265-8. doi: 10.1034/j.1600-079x.2003.00039.x.
- Van Dolah FM. Marine algal toxins: origins, health effects, and their increased occurrence. *Environ Health Perspect*. 2000;108(Suppl 1):133-41. doi: 10.1289/ehp.00108s1133.
- Vieira AC, Rubiolo JA, López-Alonso H, Cifuentes JM, Alfonso A, Bermúdez R, et al. Oral toxicity of okadaic acid in mice: study of lethality, organ damage, distribution and effects on detoxifying gene expression. *Toxins (Basel)*. 2013;5:2093-108. doi: 10.3390/toxins5112093.
- Wang J, Wang YY, Lin L, Gao Y, Hong HS, Wang DZ. Quantitative proteomic analysis of okadaic acid treated mouse small intestines reveals differentially expressed proteins involved in diarrhetic shellfish poisoning. *J Proteomics*. 2012;75:2038-52. doi: 10.1016/j.jprot.2012.01.010.
- Wang J, Lin L, Wang D-Z. Quantitative proteomic analysis reveals novel insights into hepatic toxicity in mice exposed chronically to okadaic acid. *Sci Total Environ*. 2021;775:145772. doi: 10.1016/j.scitotenv.2021.145772.
- Wuerger LTD, Hammer HS, Hofmann U, Kudiabor F, Sieg H, Braeuning A. Okadaic acid influences xenobiotic metabolism in HepaRG cells. *EXCLI J*. 2022;21:1053-65. doi: 10.17179/excli2022-5033.
- Wuerger LTD, Kudiabor F, Alarcan J, Templin M, Poetz O, Sieg H, et al. Okadaic acid activates JAK/STAT signaling to affect xenobiotic metabolism in HepaRG cells. *Cells*. 2023;12(5):770. doi: 10.3390/cells12050770.